Proceedings of the 20th International Conference on Soil Mechanics and Geotechnical Engineering– Rahman and Jaksa (Eds)

Water-retention and shear-strength characteristics of unsaturated fine-grained soils with dual-porosity microfabrics

Caractéristiques de rétention d'eau et de résistance au cisaillement des sols non-saturés à grains fins avec des microfabriques à double-porosité

Zhiqiang Lin, Jiangu Qian & Zhenhao Shi
Department of Geotechnical Engineering, Tongji University, Shanghai, 200092, China, 1710727@tongji.edu.cn

ABSTRACT: Dual-porosity microfabrics can affect the hydro-mechanical characteristics of unsaturated fine-grained soils. This work first presents an experimental study on the soil-water retention curve (SWRC) of Nanyang expansive soils. The mercury intrusion test is used to correlate macroscopic hydraulic responses to soil microstructures. Test data show the samples with dual-porosity microfabrics exhibit bimodal SWRC. Initial void ratio mainly affects inter-aggregate pore sizes and the part of SWRCs in low suction range. We further present a bimodal SWRC equation for fine-grained soils. This model discriminates capillary and adsorptive water-retention mechanisms and accounts for the effects of dual-porosity on capillary water. The last part of this paper employs suction stress concept to examine the uniqueness of strength parameters for dual-porosity soils under various suctions. In contrast to the unsaturated soils with single pore mode, the dual-porosity soils display bi-linear strength envelop and thus unique strength properties cannot be defined. Our analyses indicate that the transition in the regimes characterized by different strength properties can correspond to the transition from capillary-dominated water-retention regime to adsorptive-dominated one.

RÉSUMÉ: Les microfabriques à double-porosité peuvent affecter les caractéristiques hydromécaniques des sols non-saturés à grains fins. Ce travail présente d'abord une étude expérimentale sur la courbe de rétention d'eau (SWRC) des sols expansifs de Nanyang. Le test d'intrusion de mercure est utilisé pour corréler les réponses hydrauliques macroscopiques aux microstructures du sol. Les données de test montrent que les échantillons avec des microfabriques à double-porosité présentent une SWRC bimodale. L'indice de vide initial affecte principalement la taille des pores inter-agrégats et la partie des SWRC dans la plage de faible succion. Nous présentons ensuite une équation de SWRC bimodale pour les sols à grains fins. Ce modèle distingue les mécanismes capillaires et adsorbants de rétention d'eau et tient compte des effets de la double-porosité sur l'eau capillaire. La dernière partie de cet article utilise un nouveau concept de contrainte pour examiner l'unicité des paramètres de résistance pour les sols à double-porosité sous diverses succions. Contrairement aux sols non-saturés à simple-porosité, les sols à double-porosité présentent une enveloppe de résistance bi-linéaire et, par conséquent, des propriétés de résistance uniques ne peuvent pas être définies. Nos analyses indiquent que la transition dans les régimes caractérisés par des propriétés de résistance différentes peut correspondre à la transition d'un régime de rétention d'eau dominé par capillaire à un régime dominé par adsorption.

KEYWORDS: unsaturated soil mechanics, fine-grained soils, dual-porosity, soil-water retention curve, shear strength.

1 INTRODUCTION

The peculiarity of unsaturated soils and its importance for engineering applications have been widely recognized in the field of geotechnical engineering. The water-retention and shear-strength characteristics are fundamental to unsaturated soils, which strongly depend on the pore structure of soils. Fine-grained soils (in particular those composed of active minerals) can have two distinct types of pores: inter- and intra-aggregate pores (Delage et al. 1996, Alonso et al. 1999, Miao et al. 2002, Sun et al. 2016). The former refers to those formed between particle aggregates, whereas the latter refers to those within clay platelet clusters. The soil-water and shear-strength characteristics of the fine-grained soils with dual-porosity structures are the focus of this work.

The effects of dual-porosity structures on the soil-water characteristics have been recognized for cohesionless soils with gapped gradations (Zhang and Chen 2005, Satyanaga et al. 2013, Li et al. 2014, Wijaya and Leong 2016). These previous studies show that the SWRCs of the soils with bimodal pore-size distributions can display features that are significantly different than those assumed in conventional models (e.g., Van Genuchten 1980, Fredlund and Xing 1994). Recently reported experimental evidence suggests that dual-porosity microfabrics of fine-grained soils can also noticeably affect their abilities to retain water. For example, bimodal type of pore-size distributions has been reported (Sun et al. 2016) for Guilin lateritic clay. The corresponding SWRC shows two stages of rapid drop of water contents connected by a transitional plateau, which physically are related to the consecutive air invasion into the inter- and intra-aggregate pores as suction increases. Recent studies show that accurate modeling of SWRC for fine-grained soils, in particular, in high suction range, requires explicitly distinguishing these two fundamental mechanisms of capillarity and adsorption (Revil and Lu 2013, Konrad and Lebeau 2015, Lu 2016, Zhou et al. 2016). Many SWRC models proposed to account for capillary and adsorptive mechanisms, however, do not consider the effects of dual-porosity (Konrad and Lebeau 2015, Lu 2016, Zhou et al. 2016).

Macroscopic skeleton stress or effective stress measure that controls the deformation and failure of unsaturated soils has been an intensively debated area. One focus within this area is the inclusion of suction to skeleton stress. The suction stress concept has been found to be useful to upscale pore-scale suction to macroscopic stress that is further included into skeleton stress (Lu and Likos 2006, Likos et al. 2019). The suction stress can be defined in different ways, where the total degree of saturation (Bishop 1959), the effective degree of saturation (Han and Vanapalli 2016, Zhang et al. 2020) or the capillary degree of saturation (Konrad and Lebeau 2015, Zhou et al. 2016) can be used to upscale suction. Existing studies (Lu and Likos 2006, Alsherif and McCartney 2015, Konrad and Lebeau 2015, Ma et al. 2019, Yao et al. 2020, Zhang and Lu 2020) show that the critical state lines become unique for soils under different suctions, and thus indicating that unique and intrinsic shear strength properties can be defined for soils at different degree of saturation (fully and partially saturated sates). These studies, nevertheless, have been focused on the soils with unimodal SWRC. There are seldom counterpart studies for the dual-porosity unsaturated soils (Zhao et al. 2013, Satyanaga and Rahardjo 2019).

This paper presents a study on the water-retention and shear-strength characteristics of fine-grained soils with dual porosity microfabrics. Firstly, we discuss an experiment conducted to test the water-retention behavior of Nanyang expansive soils characterized by dual-porosity microstructures. Mercury intrusion porosimetry (MIP) tests are used to correlate the hydraulic responses and soil pore structures. Secondly, an SWRC equation is proposed for fine-grained soils, where the effects of dual-porosity structures and capillary-adsorptive mechanisms are accounted for. Lastly, the concept of suction stress is employed to study the shear strength characteristics of unsaturated soils with bimodal SWRC. We will show that the aforementioned uniqueness on shear strength parameters is lost. Rather, bi-linear strength envelop is observed that corresponds to the two regimes respectively dominated by capillary and adsorptive mechanism.

2 WATER-RETENTION TESTS ON NANYANG EXPANSIVE SOIL

The soil samples used in this test are taken from Nanyang, China. Based on its Atterberg limits (liquid limit=45.1, plastic limit=19.8), the tested soils can be classified as lean clay (CL) according to the designation of the Unified Soil Classification System (USCS). MIP tests are conducted to investigate the microstructures of specimens prepared by using two methods. Fig. 1 (a) shows the pore-size distribution (PSD) for reconstituted sample, while that of compacted samples with different void ratios is given in Fig. 1 (b).

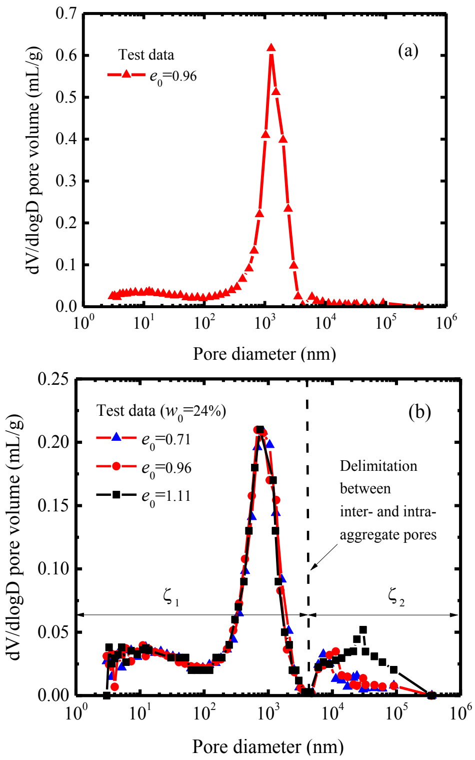

Fig. 1 PSD curves of Nanyang expansive soils: (a) reconstituted sample, (b) compacted samples with different void ratios.

It is seen that the PSD of the compacted sample shows dual-porosity characteristics, while the reconstituted specimen displays unimodal PSD. Fig. 1 (b) indicates that the change of void ratio mainly affects the inter-aggregate pore sizes. Similar behavior has been observed by Cai et al. (2020) and Sun et al. (2016).

Three suction control/measurement methods are jointly used to study the water-retention behavior of the Nanyang expansive soil over a wide suction range: axis translation technique (ATT) for low suction range (0-200 kPa), filter paper method (FPM) for medium suction range (100 kPa-8 MPa), and vapor equilibrium technique (VET) for high suction range (3.29-198.14 MPa).

Fig. 2 presents the SWRCs of compacted and reconstituted samples. It is seen that the former and latter specimens show bimodal and unimodal characteristics, respectively. In particular, the bimodal SWRCs display two stages of rapid drop of degree of saturation connected by a transitional plateau, which physically can be related to the consecutive air invasion into the inter- and intra-aggregate pores as suction increases. This double S-shape of SWRC pattern can be related to the dual-porosity structure and bimodal PSD, as shown in Fig. 1 (b). Moreover, Fig. 2 (b) indicates that the initial void ratio mainly affects the part of SWRC in low suction range, which is consistent with the aforementioned observations on soil microstructures, i.e., the change of void ratio mainly affects the inter-aggregate pore sizes.

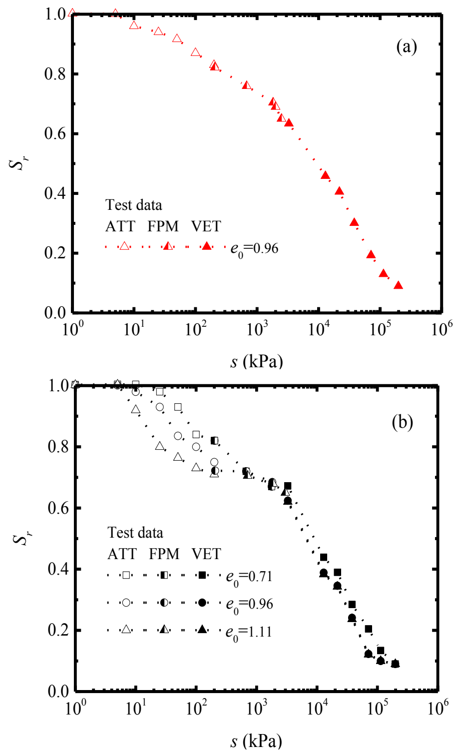

Fig. 2 SWRCs of Nanyang expansive soils: (a) reconstituted sample, (b) compacted samples with different void ratios.

3 BIMODAL SOIL-WATER RETENTION CURVE EQUATION

To account for the dual-porosity microfabrics of fine-grained soils, a new SWRC equation is proposed. The model considers the additive decomposition of the total degree of saturation into capillary and adsorptive parts:

$$S_r = S_r^{cap} + S_r^{ads} \quad (1)$$

$$S_r^{cap} = (1-\alpha)A(s) + (\alpha - S_r^{ads})B(s) \quad (2)$$

$$S_r^{ads} = C(s)(\alpha - S_r^{ads})(1 - B(s)) \quad (3)$$

where S_r^{cap} and S_r^{ads} denote the capillary and adsorptive degree of saturation, respectively, while s indicates suction.

In the capillary water retention curve of Eq. (2), $\alpha = \theta_{s2}/\theta_{s1}$, where the variables θ_{s1} and θ_{s2} indicate the volumetric moisture contents that correspond to the air-entry value of the inter- and intra-aggregate pore, respectively (see Fig. 3). Accordingly, $(1-\alpha)$ indicates the capillary water content of the completely filled inter-aggregate pores, while $(\alpha - S_r^{ads})$ gives the capillary water content of the completely filled intra-aggregate pores. The functions $A(s)$ and $B(s)$ in Eq. (2) are related to the distribution of the inter- and intra-aggregate pore sizes, respectively, in a way similar to unimodal SWRC equations (e.g., Khlosi et al. 2008, Zhou et al. 2016):

$$A(s) = \left[\frac{1}{2} erfc\left(ln\left(\frac{s}{s_{m1}}\right)/\sqrt{2}\zeta_1\right)\right] \tag{4}$$

$$B(s) = \left[\frac{1}{2} erfc\left(ln\left(\frac{s}{s_{m2}}\right)/\sqrt{2}\zeta_2\right)\right] \tag{5}$$

where s_m denotes the suction corresponds to the median pore size, while ζ is the standard deviation of the log-transformed pore radium (see Fig. 1). Here the subscripts 1 and 2 indicate the quantities associated with the inter- and intra-aggregate pores, respectively. The symbol $erfc()$ in Eqs. (4) and (5) denotes the complementary error function.

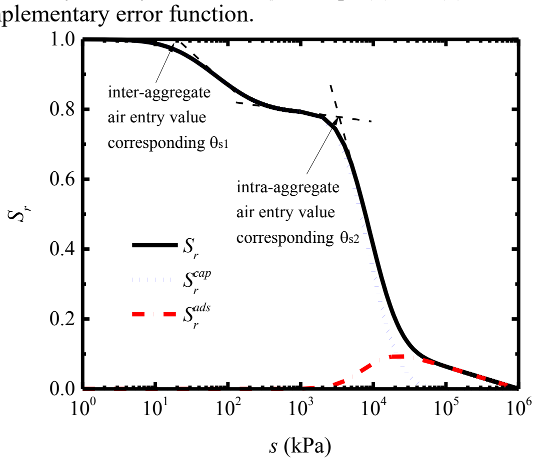

Fig. 3 Schematic illustration of the proposed bimodal SWRC equation.

In the adsorptive water retention curve of Eq. (3), the functions $C(s)$ describes a log-linear reduction of the degree of saturation with suction near oven-dry conditions:

$$C(s) = \beta\left(1 - \frac{lns}{lns_d}\right) \tag{6}$$

where β is a material parameter that indicates the change rate of adsorptive saturation in high suction range, s_d (1×10^6 kPa) indicates the maximum suction under oven-dry conditions. The term $(\alpha - S_r^{ads})(1-B(s))$ in Eq. (3) is introduced to consider intra-aggregate capillary condensation, that is, the intra-aggregate adsorptive water tends to transform to capillary water when the thickness of water film reaches a critical value as suction decreases. It is seen from Fig. 3 that, as suction decreases, the adsorbed water reaches a peak. After it, the adsorbed water gradually decreases to zero as the suction approaches the intra-aggregate air entry value.

Fig. 4 compares the water-retention test data of M6, M8, Guilin lateritic clay (Satyanaga 2015, Sun et al. 2016, Satyanaga and Rahardjo 2019) and Nanyang expansive soil and those computed by the aforementioned SWRC equation. These four fine-grained soils are characterized by dual-porosity microfabrics.

It is seen from Fig. 4 that the computed SWRCs can well represent the bimodal water-retention behavior of fine-grained soils, e.g., two stages of rapid drop of degree of saturation connected by a transitional plateau. In Fig. 4, the proposed SWRC model is used to further inspect the potential variation of different types of soil water during drying process (see the CWRC (capillary water retention curve) and AWRC (adsorbed water retention curve)). These computations suggest that the inter-aggregate pores first lose capillary water as suction increases. During the subsequent drying process, the intra-aggregate pores began to lose capillary water. Simultaneously, part of the capillary water is transformed into adsorbed water. The adsorbed water displays a bounded peak, after which gradually decreases to zero as the oven-dry conditions are approached.

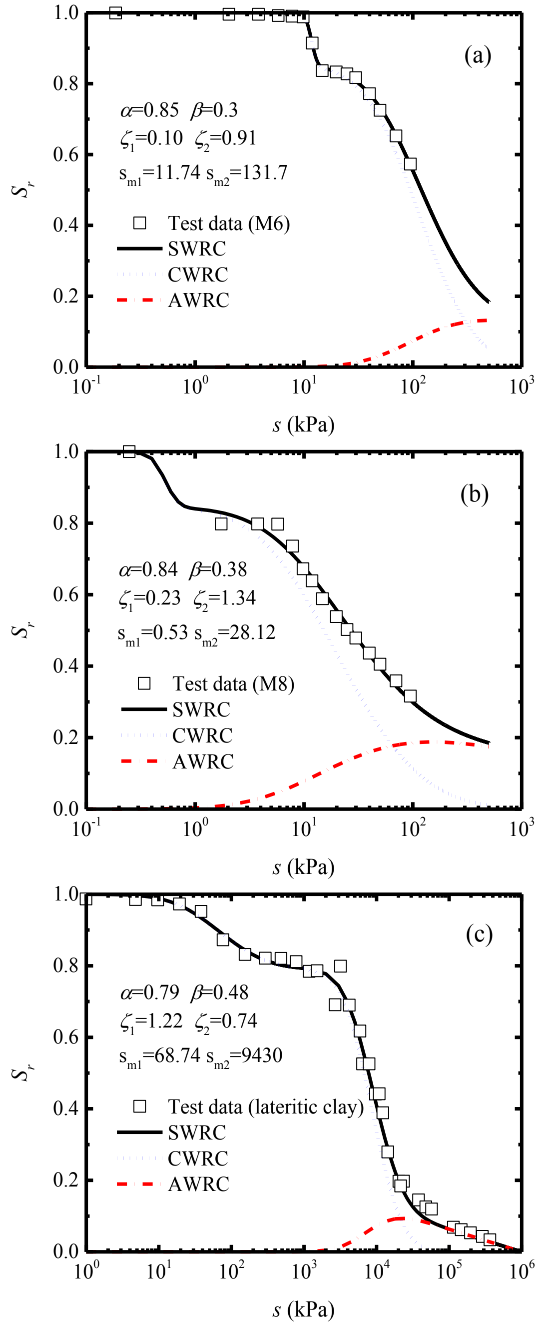

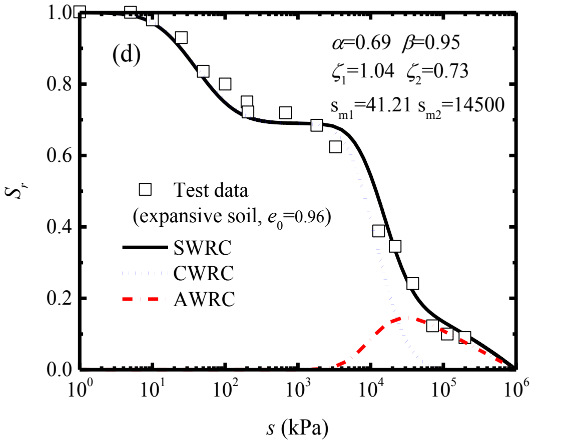

Fig. 4 Comparison between measured and computed SWRC for fine-grained soils with dual porosity microfabrics: (a) M6 clay, (b) M8 clay, (c) Guilin lateritic clay and (d) Nanyang expansive soil (data from Satyanaga 2015, Sun et al. 2016, Satyanaga and Rahardjo 2019)

4 STRENGTH CHARACTERISTICS OF FINE-GRAINED SOILS WITH DUAL-POROSITY

Figure 5 shows the shear strength of the fine-grained soils studied in section 3 under different suctions. Non-linear relationships can be clearly observed. Existing studies indicate that the soils under different suctions can be characterized by a single failure line and consequently unique shear strength properties, provided that appropriate suction stress is included in skeleton stress measure.

In the following, we first use the total degree of saturation to upscale the pore suction to define macroscopic suction stress ($S_r\ s$). For this purpose, the calibrated SWRC equation in Fig. 4 is used. The data depicted in Fig. 5 are re-plotted as the relationships between shear strength and suction stress in Fig. 6. It is seen that the shear strength still varies non-linearly with the suction stress. This feature is in contrast to that observed for coarse-grained soils (Bishop et al. 1960, Fredlund and Rahardjo 1993), and indicates that, for fine-grained soils, the upscaling based on the total degree of saturation might not reasonably reflect the contribution of suction to skeleton stress and the consequent shear strength.

As discussed in recently published studies (Zhou et al. 2016, Zhang and Lu 2020), one potential reason for the failure to identify unique failure line in shear strength and suction stress $S_r\ s$ space is that, for fine-grained soils, the adsorbed water does not contribute to the shear strength. This type of soil water is mainly stored in intra-aggregate pores, whereas the inter-contacts between aggregates can constitute the origins of the resistance of bulk materials to distortion. Following existing studies (Baker and Frydman 2009, Fuentes and Triantafyllidis 2013, Konrad and Lebeau 2015, Zhou et al. 2016), we employ capillary saturation (S_r^{cap}) to upscale pore-scale suction and define the suction stress $S_r^{cap}s$. Figs. 7 and 8 show the relationships between shear strength and the suction stress $S_r^{cap}s$. The shear strength tends to vary linearly with the suction stress. This indicates that the soil water retained via capillarity might govern the contribution of pore-scale suction to the macroscopic skeleton stress of unsaturated soils, as also reported by the existing studies for the soils with unimodal SWRC (e.g., Konrad and Lebeau 2015, Zhou et al. 2016).

On the other hand, differing from these studies, Figs. 7 and 8 show that the strength envelops for the dual-porosity soils display a bi-linear pattern. The slope of the failure line is different between the suction regimes where the suction stress $S_r^{cap}s$ increases and decreases with the suction, respectively (see the non-monotonic variation of $S_r^{cap}s$ with suction in Fig. 9). Comparing Fig. 9 and Fig. 4 indicates that the transition between these two suction regimes is close to the intra-aggregate air entry values. Furthermore, Fig. 3 suggests that the intra-aggregate air entry value can be the critical suction after which adsorptive water gradually emerges as suction increase further. These facts, therefore, suggest that the transition in strength characteristics shown in Figs. 7 and 8 might coincide with the transition between capillary-dominated water retention regime and adsorptive-dominated one.

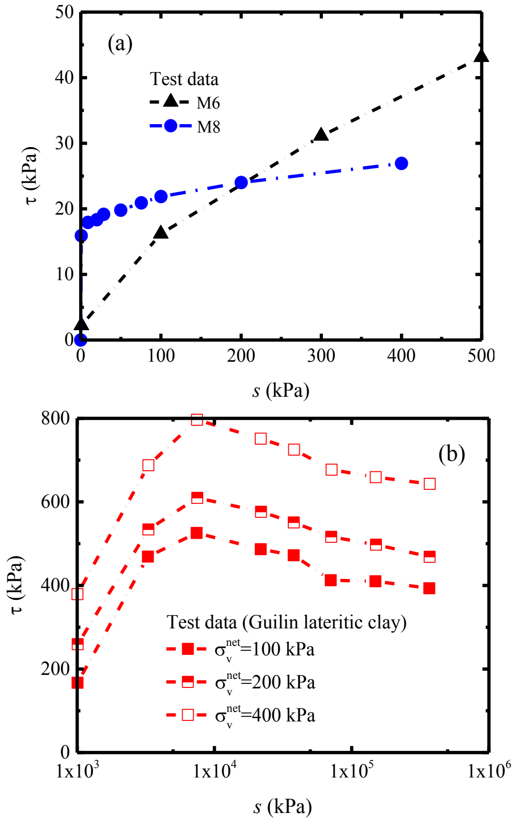

Fig. 5 Relationship between shear strength and suction for the fine-grained soils with dual-porosity microfabrics: (a) M6 and M8 clay and (b) Guilin lateritic clay under different net vertical pressures (data from Satyanaga and Rahardjo 2019; Sun et al. 2016, 2017)

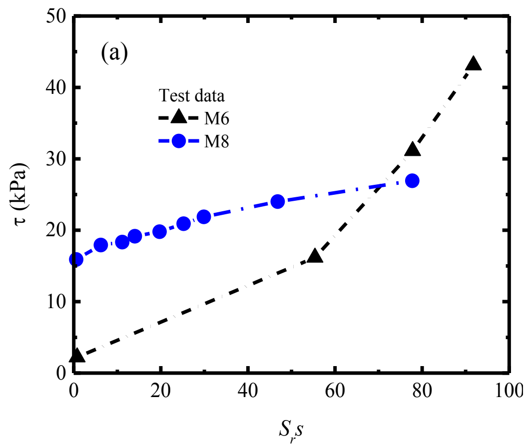

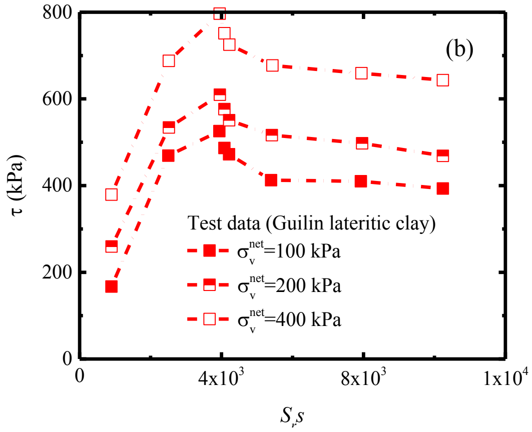

Fig. 6 Data in Fig. 5 re-plotted in shear strength and suction stress ($S_r\ s$) plane.

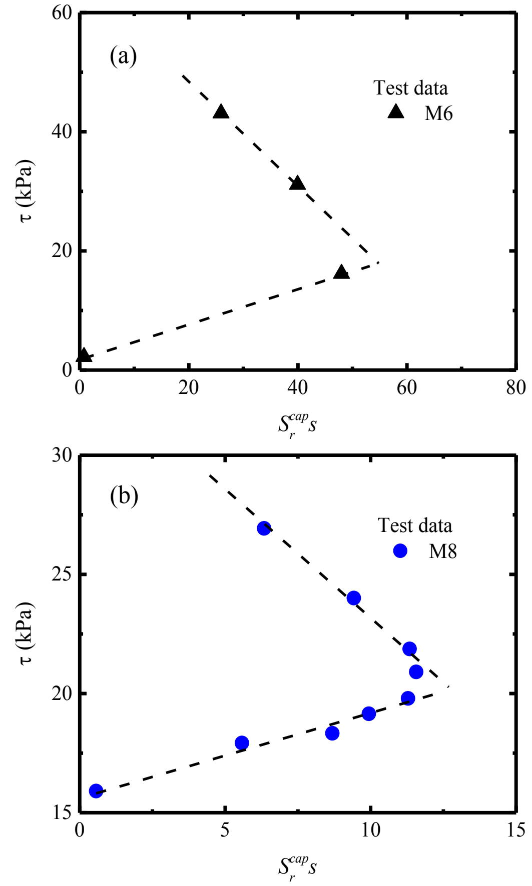

Fig. 7 Data in Fig. 5(a) re-plotted in shear strength and suction stress ($S_r^{cap}s$) plane.

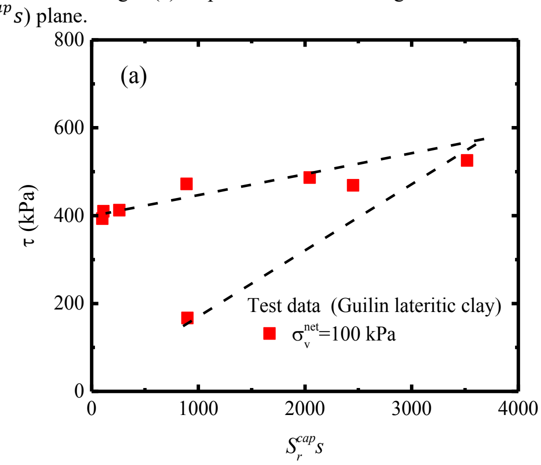

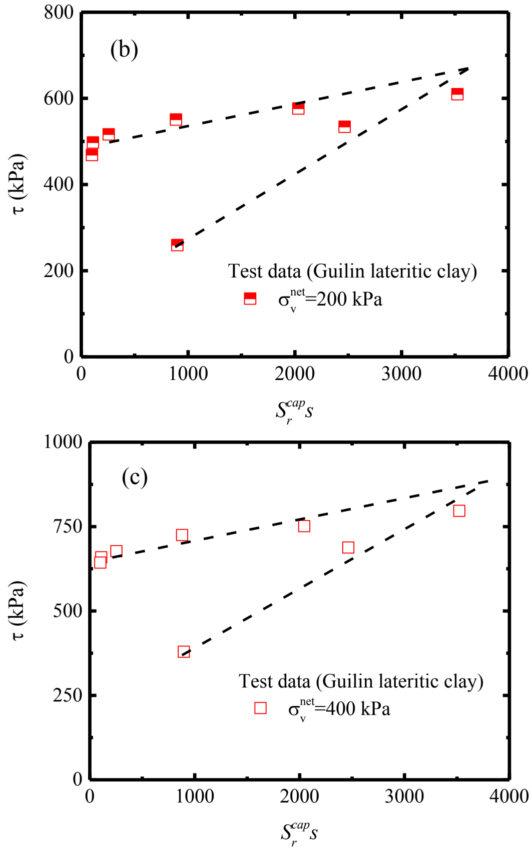

Fig. 8 Data in Fig. 5(b) re-plotted in shear strength and suction stress ($S_r^{cap}s$) plane.

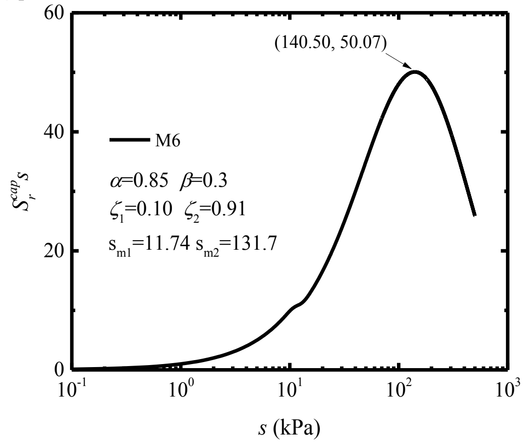

Fig. 9 Variation of suction stress $S_r^{cap}s$ with suction for M6 clay.

5 SUMMARIES AND CONCLUSIONS

This work investigates the water-retention and shear-strength characteristics of fine-grained soils with dual-porosity microfabrics. Firstly, axis translation technique (ATT), filter paper method (FPM) and vapor equilibrium technique (VET) are jointly used to study the SWRCs of Nanyang expansive soils. Mercury intrusion porosimetry (MIP) is employed to examine the microstructures of soils. Test data indicate that the compacted samples display dual-porosity microstructures and the corresponding SWRCs show bimodal patterns. Initial void ratio mainly affects the inter-aggregate pore sizes and consequently the part of SWRCs in low suction range.

An SWRC equation is proposed for fine-grained soils, where water-retention mechanisms via capillarity and adsorption are explicitly distinguished. The effects of dual-porosity on the capillary water are included. This model can reasonably represent the bimodal water-retention behavior of the tested soils and those reported in the literature.

The concept of suction stress is used to examine the strength characteristics of the dual-porosity soils. For fine-grained soils, the capillary degree of saturation is more appropriate to upscale pore-scale suction to macroscopic suction stress that directly contributes to shear strength. The strength envelop of the dual-porosity soils displays bi-linear relationships against the suction stress, indicating the unique strength parameters can be defined, unlike the soils with unimodal SWRC. The transition in the regimes characterized by different strength characteristics corresponds to the transition from capillary-dominated water-retention regime to adsorptive-dominated one.

6 ACKNOWLEDGEMENTS

This work is supported by the National Natural Science Foundation of China through Grant No. 41877252.

7 REFERENCES

Alonso, E.E., Vaunat, J., and Gens, A. 1999. Modelling the mechanical behaviour of expansive clays. Engineering Geology, **54**(1–2): 173–183. doi:10.1016/S0013-7952(99)00079-4.

Alsherif, N.A., and McCartney, J.S. 2015. Thermal behaviour of unsaturated silt at high suction magnitudes. Geotechnique, **65**(9): 703–716. doi:10.1680/geot.14.P.049.

Baker, R., and Frydman, S. 2009. Unsaturated soil mechanics. Critical review of physical foundations. Engineering Geology, **106**(1–2): 26–39. doi:10.1016/j.enggeo.2009.02.010.

Bishop, A.W. 1959. The principle of effective stress. Teknik Ukeblad,.

Bishop, A.W., Alpan, I., Blight, G.H., and Donald, I.B. 1960. Factors controlling the strength of partly saturated cohesive soils. *In* Proceedings of the ASCE Research Conference on Shear Strength of Cohesive Soils. pp. 503–532.

Cai, G., Zhou, A., Liu, Y., Xu, R., and Zhao, C. 2020. Soil water retention behavior and microstructure evolution of lateritic soil in the suction range of 0–286.7 MPa. Acta Geotechnica, **15**(12): 3327–3341. doi:10.1007/s11440-020-01011-w.

Delage, P., Audiguier, M., Cui, Y.J., and Howat, M.D. 1996. Microstructure of a compacted silt. Canadian Geotechnical Journal, **33**(1): 150–158. doi:10.1139/t96-030.

Fredlund, D.G., and Rahardjo, H. 1993. Soil mechanics for unsaturated soils. *In* John Wiley & Sons, Inc.

Fredlund, D.G., and Xing, A. 1994. Equations for the soil-water characteristic curve. Canadian geotechnical journal, **31**(4): 521–532.

Fuentes, W., and Triantafyllidis, T. 2013. On the effective stress for unsaturated soils with residual water. Geotechnique, **63**(16): 1451–1455. doi:10.1680/geot.13.T.013.

Van Genuchten. 1980. A closed-form equation for predicting the hydraulic conductivity of unsaturated soils. Soil Science Society of America Journal, **17**(4): 892–898. doi:10.1016/j.pan.2017.07.214.

Han, Z., and Vanapalli, S.K. 2016. Stiffness and shear strength of unsaturated soils in relation to soil-water characteristic curve. Geotechnique, **66**(8): 627–647. doi:10.1680/jgeot.15.P.104.

Khlosi, M., Cornelis, W.M., Douaik, A., van Genuchten, M.T., and Gabriels, D. 2008. Performance evaluation of models that describe the soil water retention curve between saturation and oven dryness. Vadose Zone Journal, **7**(1): 87–96. doi:10.2136/vzj2007.0099.

Konrad, J.M., and Lebeau, M. 2015. Capillary-based effective stress formulation for predicting shear strength of unsaturated soils. Canadian Geotechnical Journal, **52**(12): 2067–2076. doi:10.1139/cgj-2016-0101.

Li, X., Li, J.H., and Zhang, L.M. 2014. Predicting bimodal soil-water characteristic curves and permeability functions using physically based parameters. Computers and Geotechnics, **57**: 85–96. doi:10.1016/j.compgeo.2014.01.004.

Likos, W.J., Song, X., Xiao, M., Cerato, A., and Lu, N. 2019. Fundamental challenges in unsaturated soil mechanics. Springer International Publishing.

Lu, N. 2016. Generalized soil water retention equation for adsorption and capillarity. Journal of Geotechnical and Geoenvironmental Engineering, **142**(10): 04016051. doi:10.1061/(asce)gt.1943-5606.0001524.

Lu, N., and Likos, W.J. 2006. Suction stress characteristic curve for unsaturated soil. Journal of Geotechnical and Geoenvironmental Engineering, **132**(2): 131–142. doi:10.1061/(asce)1090-0241(2006)132:2(131).

Ma, T., Wei, C., Chen, P., and Li, W. 2019. Chemo-mechanical coupling constitutive model for chalk considering chalk-fluid physicochemical interaction. Geotechnique, **69**(4): 308–319. doi:10.1680/jgeot.17.P.115.

Miao, L., Liu, S., and Lai, Y. 2002. Research of soil-water characteristics and shear strength features of Nanyang expansive soil. Engineering Geology, **65**(4): 261–267. doi:10.1016/S0013-7952(01)00136-3.

Revil, A., and Lu, N. 2013. Unified water isotherms for clayey porous materials. Water Resources Research, **49**(9): 5685–5699. doi:10.1002/wrcr.20426.

Satyanaga, A. 2015. Soil water characteristic curve and shear strength of soil with bimodal characteristic (PhD thesis).

Satyanaga, A., and Rahardjo, H. 2019. Unsaturated shear strength of soil with bimodal soil-water characteristic curve. Geotechnique, **69**(9): 828–832. doi:10.1680/jgeot.17.P.108.

Satyanaga, A., Rahardjo, H., Leong, E.C., and Wang, J.Y. 2013. Water characteristic curve of soil with bimodal grain-size distribution. Computers and Geotechnics, **48**(10): 51–61. doi:10.1016/j.compgeo.2012.09.008.

Sun, D., You, G., Annan, Z., and Daichao, S. 2016. Soil–water retention curves and microstructures of undisturbed and compacted Guilin lateritic clay. Bulletin of Engineering Geology and the Environment, **75**(2): 781–791. doi:10.1007/s10064-015-0765-2.

Sun, D.A., He, J.H., and Gao, Y. 2017. Strength characteristics of compacted lateritic clay in a wide range of suction. Yantu Lixue/Rock and Soil Mechanics, **38**(2): 51–56. doi:10.16285/j.rsm.2017.S2.007.

Wijaya, M., and Leong, E.C. 2016. Equation for unimodal and bimodal soil-water characteristic curves. Soils and Foundations, **56**(2): 291–300. Elsevier. doi:10.1016/j.sandf.2016.02.011.

Yao, C., Chen, P., Ma, T., Xia, X., and Wei, C. 2020. Physicochemical effect on shear strength characteristics of clayey soils based on ring-shear experiment. Canadian Geotechnical Journal, **57**(12): 1820–1831. doi:10.1139/cgj-2019-0513.

Zhang, C., and Lu, N. 2020. Unified effective stress equation for soil. Journal of Engineering Mechanics, **146**(2): 04019135. doi:10.1061/(asce)em.1943-7889.0001718.

Zhang, J., Niu, G., Li, X., and Sun, D. 2020. Hydro-mechanical behavior of expansive soils with different dry densities over a wide suction range. Acta Geotechnica, **15**(1): 265–278. Springer Berlin Heidelberg. doi:10.1007/s11440-019-00874-y.

Zhang, L., and Chen, Q. 2005. Predicting bimodal soil–water characteristic curves. Journal of Geotechnical and Geoenvironmental Engineering, **131**(5): 666–670. doi:10.1061/(asce)1090-0241(2005)131:5(666).

Zhao, H.F., Zhang, L.M., and Fredlund, D.G. 2013. Bimodal shear-strength behavior of unsaturated coarse-grained soils. Journal of Geotechnical and Geoenvironmental Engineering, **139**(12): 2070–2081. doi:10.1061/(asce)gt.1943-5606.0000937.

Zhou, A., Huang, R., and Sheng, D. 2016. Capillary water retention curve and shear strength of unsaturated soils. Canadian Geotechnical Journal, **53**(9): 974–987. doi:10.1051/e3sconf/20160914010.